Histochemical Structure and Tensile Properties of Birch Cork Cell Walls

Shingo Kiyoto
Kyoto University Graduate School of Agriculture Faculty of Agriculture: Kyoto Daigaku Nogaku Kenkyuka Nogakubu

Junji Sugiyama (sugiyama.junji.6m@kyoto-u.ac.jp)
Kyoto University Graduate School of Agriculture Faculty of Agriculture: Kyoto Daigaku Nogaku Kenkyuka Nogakubu https://orcid.org/0000-0002-5388-4925

Research Article

Keywords: Cellulose, Cork, Polarizing light microscopy, Suberin, Transmission electron microscopy

Posted Date: March 23rd, 2021

DOI: https://doi.org/10.21203/rs.3.rs-327370/v1

Version of Record: A version of this preprint was published at Cellulose on July 12th, 2021. See the published version at https://doi.org/10.1007/s10570-021-04036-w.

Abstract

Tensile tests of birch cork were performed in the tangential direction. Birch cork in the wet state showed significantly higher extensibility and toughness than those in the oven-dried state. The histochemical structure of birch cork was investigated by microscopic observation and spectroscopic analysis. Birch cork cell walls showed a three-layered structure. In transmission electron micrographs, osmium tetroxide stained the outer and inner layers, whereas potassium permanganate stained the middle and inner layers. After chemical treatment to remove suberin and lignin, the outer and inner layers disappeared and Fourier-transformed infrared spectra showed the cellulose I pattern. Polarizing light micrographs indicated that molecular chains in the outer and inner layers were oriented perpendicular to suberin lamination, whereas those in the inner layer showed longitudinal orientation. These results suggested that the outer and inner layers mainly consist of suberin, whereas the middle layer and compound middle lamella consist of lignin, cellulose, and other polysaccharides. We hypothesized a hierarchical model of the birch cork cell wall. The lignified cell wall with helical arrangement of cellulose microfibrils is sandwiched between two suberized walls. Cellulose microfibrils in the middle layer act like a spring and bear tensile loads. In the wet state, water and cellulose in the compound middle lamella transfer tensile stress between cells. In the dried state, this stress-transferal system functions poorly and fewer cells bear stress. Suberin in the outer and inner layers prevents absolute drying to maintain mechanical properties of the bark and to bear tensile stress caused by trunk diameter growth.

Introduction

Cork is the outermost tissue of the bark and plays an important role in protecting the tree body owing to its thermal insulation, pest resistance, and water repellency. To confer these properties, cork cell walls have a distinct chemical constitution and anatomical structure from those of other tissues. The most important characteristic of the cork cell wall is a high content of suberin. Suberin is an aliphatic-aromatic crosslinked polyester (Gardini et al. 2006). Several properties of cork, such as thermal stability, originate from the presence of suberin (Pereira 2015). Cork from a number of woody species has been used for its useful properties. Mechanical properties of cork differ among tree species because of differences in anatomical structure and results in different industrial usages.

The most popularly used cork is that from *Quercus suber*. It has been used as a bottle stopper on account of its low density, impermeability to water and gases, high compressive strength, and dimensional recovery. These properties reflect the cell size and structure of the hexagonal prism (Gibson et al. 1981). Cherry cork has been used as a Japanese traditional craft (“Kabazaiku”) because of its smooth surface and beautiful glossy, dark red color. In addition, the mechanical properties of cherry cork are notable: extensibility greater than 120%, Young’s modulus 0.9–1.6 GPa, and toughness approximately 40 GPa in the tangential direction (Kobayashi et al. 2018; Xu et al. 1997). These values surpass the tensile properties of *Q. suber* cork (Anjos et al. 2008; 2010). The tensile properties are due to the tangentially elongated cell shape and aligned cell wall fibers (Xu et al. 1997). Birch cork has been used as a traditional craft in Russia and is noted for its toughness and water resistance. The anatomical structure and

seasonal growth of birch cork has been investigated previously (Shibui and Sano 2018; Schönherr and Ziegler 1980; Bhat 1982). However, to the best of our knowledge, few studies have been conducted on the histochemical structure of the cell wall and the mechanical properties of birch cork for its limited industrial uses, despite the broad distribution of birch on the Eurasian continent.

In this report, we performed tensile tests and surveyed the histochemical structure of birch cork using polarizing light microscopy (PLM) and transmission electron microscopy (TEM). From the insights obtained from these experiments, we discuss the relationship between the histochemical structure and mechanical properties of the cell wall of birch cork.

Materials And Methods

Plant materials

Outer bark was stripped from a birch tree (*Betula platyphylla*) growing in national forests in Gifu prefecture on 20 June 2014. The diameter at breast height of the sampled tree was 26 cm. The innermost portion of the bark (approximately 300 μm thick) was stripped and air-dried, and was subsequently subjected to tensile tests, spectroscopic analysis, or microscopic observation.

Tensile test

A dumbbell-type strip of bark, with the dimensions 5 mm (L) × 0.2 mm (R, calibrated with a micrometer for each sample) × 30 mm (T), was trimmed with a metal mold for the tensile test. The air-dried samples were kept conditioned at room temperature. A portion of samples were oven-dried at 120 °C overnight and returned to room temperature in a desiccator containing silica gel for 6 h. Some samples were hydrated by de-aeration in water. Tensile tests in tangential directions were performed on 10 specimens per sample, with span length 20 mm and crosshead speed 10 mm min^{-1}, with a testing machine (LSC-1, Tokyo Kouki, Tokyo, Japan).

Chemical treatment for removal of suberin and lignin

To observe the cellulosic material in the cork cell wall, suberin and lignin were removed by alkali ethanolysis and the Wise method, respectively. Suberin was removed from some samples in accordance with the method reported by Ekman and Eckerman (1985) with slight modification: the samples were hydrolyzed with 0.5 N KOH in 90% ethanol at 80 °C for 2 h without stirring. After washing repeatedly in distilled water, the samples were subjected to delignification via sodium chlorite oxidation in water at pH 4.8 at 70 °C for 1 h. The products were washed repeatedly in distilled water. Fourier-transformed infrared (FTIR) spectra were obtained from samples for each procedure using a FTIR spectrometer (Frontier, Perkin-Elmer, Waltham, MA, USA). Samples before and after chemical treatment were subjected to pretreatments for microscopic observation.

Sample preparation for microscopic observation

Birch cork samples were cut into small blocks. Some of the samples were stained *en bloc* with 1% osmium tetroxide (OsO_4) in 0.1 M phosphate buffer or with 1% aqueous solution of potassium permanganate ($KMnO_4$) in 0.1% sodium citrate for 2 h at room temperature, and washed repeatedly with distilled water. These blocks were dehydrated through an ethanol series (up to 99.5% ethanol). The blocks were embedded in Spurr's resin. Some blocks were substituted with xylene and embedded in paraffin. Some blocks after removal of suberin and lignin were substituted with propylene oxide and embedded in Epon812 resin.

Polarizing light microscopic observation

Radial and transverse sections (each 5 μm thick) were cut from cork samples embedded in Spurr's resin before and after chemical treatment as described above. To determine molecular chain orientation from the polarization color, sections without chemical treatment were bleached by sodium chlorite oxidation in water at pH 4.8 at 70 °C for 1 h. These sections were stained using the periodic acid–Schiff reaction (PAS). Sections from the samples after removal of suberin and lignin were observed without staining. Sections were mounted with Bioleit mounting medium (Oken-shoji, Tokyo, Japan) and observed with a PLM (BX53-P, Olympus, Tokyo, Japan) equipped with a digital camera (DP74, Olympus).

Transmission electron microscopic observation

Radial and transverse ultrathin (100 nm thick) sections were cut from blocks of untreated samples before embedding. In addition, samples embedded with Epon812 resin after removal of suberin and lignin and were also cut into ultrathin radial sections. These sections were mounted on copper grids (300 mesh) and floated on a drop of 1 % aqueous solution of $KMnO_4$ in 0.1 % sodium citrate for 30 min at room temperature. Sections were washed with distilled water, dried, and observed at 80 kV with a TEM (JEM1400, JEOL, Tokyo, Japan). Samples that were embedded in Spurr's resin after staining with OsO_4 or $KMnO_4$ were also used to cut ultrathin radial sections and observed without post-staining.

Raman microscopic observation

Transverse 10-μm-thick sections were cut from paraffin-embedded blocks. Paraffin was removed from the sections with xylene, and xylene was substituted to 100% ethanol. The sections were hydrated in a graded ethanol series until water was used. The sections were mounted on glass slides in distilled water, covered with cover glass, and sealed. The Raman spectra were acquired using a micro-Raman system (LabRam Xplora, Horiba Jobin Yvon, Essonne, France) equipped with a light microscope (BX51, Olympus) and laser (λ = 638 nm). The LabSpec instrumentation software (Horiba Jobin Yvon) was used to control the micro-Raman system. Baseline correction was performed based on the airPLS algorithm using Python 3.7.4 software (Zhang et al. 2017). Brightfield micrographs were also captured.

Results

Tensile tests

Wet-state birch cork showed the highest extensibility, followed in order by air-dried and oven-dried cork (Fig. 1a). Wet-state cork showed a lower elastic modulus than cork samples in the other two states and a significantly lower tensile strength than air-dried cork (Fig. 1b). Oven-dried cork showed lower toughness than samples in the other two states.

Fourier-transformed infrared spectra

The FTIR spectra from birch bark are shown in Fig. 2. Untreated birch cork showed two strong peaks at 2929 and 2851 cm^{-1} (Fig. 2a, arrows). After suberin removal, intensity of the two peaks decreased significantly, and peaks at 1600 and 1510 cm^{-1} were observed (Fig. 2b, arrowheads). After delignification, these peaks almost disappeared (Fig. 2c).

Polarizing light microscopic observation

The PLM micrographs of radial sections from birch cork cell walls with and without degradation of suberin are shown in Fig. 3. Intact birch cork cell walls were yellow-colored (data not shown). Therefore, sections from samples without removal of suberin were also bleached using the Wise method to investigate molecular chain orientation from the polarization color. In radial sections birch cork cells were rectangular in shape with an oval lumen. The cell wall showed a three-layer structure: thick outer layer, thin and oval-shaped middle layer, and inner layer (Fig. 3a). A portion of the inner layer showed an amorphous-like structure. In addition, the compound middle lamella and middle layer were strongly stained by the PAS reaction. Under crossed-Nicol prisms, the outer and inner layers exhibited strong birefringence (Fig. 3b). Under a retardation plate, the outer and inner layers showed a blue color in the tangential wall (Fig. 3c). After degradation of suberin, the outer and inner layers disappeared, and the middle layer and compound middle lamella were observed under opened-Nicol prisms (Fig. 3d). Under crossed-Nicol prisms, the compound middle lamella and middle layer exhibited weak birefringence (Fig. 3e). Under a retardation plate, the tangential wall of the compound middle lamella and middle layer showed a yellow color (Fig. 3f).

The PLM micrographs of transverse sections from birch cork cell walls with and without degradation of suberin are shown in Fig. 4. Birch cork cells were elongated in tangential directions (Fig. 4). Under crossed-Nicol prisms, the outer layer exhibited strong birefringence (Fig. 4b). Under a retardation plate, the outer and inner layers showed a yellow color in the tangential wall. After removal of suberin, it was difficult to distinguish which layer remained under opened-Nicol prisms (Fig. 4d). Under crossed-Nicol prisms, the remaining cell wall barely showed birefringence (Fig. 4e). Under a retardation plate, the tangential wall of the remaining cell wall showed a faint yellow color (Fig. 4f).

Transmission electron microscopic observation

The TEM micrographs taken from $KMnO_4$-stained samples are shown in Fig. 5. In the sections stained after resin embedding, the compound middle lamella, middle layer, and inner layer were stained with $KMnO_4$ (Fig. 5a, d–f). The middle layer was oval-shaped in radial section (Fig. 5a) and pointed in the

longitudinal and tangential directions (Fig. 5a, e). In the samples stained before Spurr's resin embedding, only the inner layer was stained and the middle layer showed a lower electronic density than the outer layer (Fig. 5b). In the sample embedded in Epon812 resin after removal of suberin and lignin, the area other than the middle layer and compound middle lamella was stained with $KMnO_4$ (Fig. 5c).

The TEM micrographs captured from OsO_4-stained samples are shown in Fig. 6. Alternating layers of electron-dense and electron-lucent areas were observed in the outer layers of both early cork and late cork (Fig. 6a, d). The inner layer appeared thinner in early cork than in late cork (Fig. 6a, d).

Raman microscopic observation

Raman spectra obtained from birch cork cell walls are shown in Fig. 7. Spectra were obtained from the outer part of the cell wall (Fig. 7c) and amorphous-like structure of the inner part (Fig. 7d). Both spectra included two strong CH stretching bands at 2929 and 2851 cm^{-1} (Fig. 7a, b). Spectra from the outer wall showed a weak OH stretching vibration at 3440 cm^{-1} (Fig. 7a). Bands at 1600 cm^{-1} and 1640 cm^{-1} were slightly stronger in the inner wall than in the outer wall (Fig. 7a, b).

Discussion

Chemical composition and architecture of birch cork cell wall

The FTIR spectrum of untreated birch cork showed a similar pattern to those of *Prunus serrula* and *Quercus suber* (Xu et al. 1997). Two sharp CH stretching peaks at 2929 and 2851 cm^{-1} (Fig. 2a, arrows) were considered to stem from the suberin aliphatic domain. Two peaks at 1600 and 1510 cm^{-1}, which appeared after removal of suberin by alkali ethanolysis (Fig. 2b, arrowheads), originated from aromatic skeleton vibrations of lignin. After delignification using the Wise method, these peaks disappeared and the spectrum clearly showed the fingerprint region of cellulose I crystals (Fig. 2c, ellipses). Therefore, it was confirmed that these chemical treatments successfully removed suberin and lignin and that micrographs after treatment (Figs. 3d–f, 4d–f, and 5c) indicated observation of cellulose in the birch cork cell wall.

Both PLM and TEM micrographs indicated that the birch cork cell wall has a three-layered structure (Figs. 3, 5, and 6). In the OsO4-stained samples, the outer layer showed a multilayered structure with alternating electron-dense and -lucent layers (Fig. 6a, c). This pattern is typical of a suberized cell wall, as reported previously (Ryser and Holloway 1985; Serra et al. 2009; Sitte 1962; Teixeira and Pereira 2010). Therefore, birefringence in the outer wall is considered to originate from the aliphatic domain of suberin. The PLM observation with a retardation plate showed that the suberin aliphatic domain of the outer and inner layers is oriented perpendicular to the suberin lamella observed in TEM micrographs. These results agreed with previous reports indicating that the electron-lucent layers correspond to the aliphatic domain of suberin and that the molecular chain of the domain is oriented perpendicular to the suberin lamella (Schmutz et al. 1993, 1996).

The compound middle lamella and middle layer were strongly stained by the PAS reaction (Fig. 3a) and $KMnO_4$ (Fig. 5a–d). These observations indicated the presence of lignin and other polysaccharides. In the samples embedded in Epon812 resin after removal of suberin and lignin, $KMnO_4$ stained parts of the cell wall other than the compound middle lamella and middle layer (Fig. 5f). Previously, $KMnO_4$ was reported to stain methyl nadic anhydride of Epon812 resin (Reedy 1965). As mentioned above, the main component of the residue after removal of suberin and lignin is cellulose. Therefore, birefringence in PLM micrographs after the chemical treatments (Figs. 3d–f and 4d–f) indicated the orientation of cellulose microfibrils. The PLM observation with a retardation plate showed that cellulose microfibrils in the middle layer are oriented in the longitudinal direction of the tree body.

The inner layer was stained with OsO_4 similar to the outer layer (Fig. 6). However, the inner layer was stained also with $KMnO_4$, whereas the outer wall was barely stained (Fig. 5). These results implied the presence of a free phenolic hydroxyl group, which is reportedly stained with $KMnO_4$ (Bland et al. 1971). In the samples stained *en bloc* before embedding, only the inner layer was stained (Fig. 5e). This may suggest that the inner layer acts as a hydrophobic barrier between the lumen and middle layer. Raman spectra obtained from the outer and inner parts of the cork cell wall showed similar patterns (Fig. 7a, b). However, the spectrum from the outer part showed weak and broad bands at 3430 cm^{-1} and bands at 1600 and 1640 cm^{-1} were slightly stronger in the inner part than in the outer part. Bands at 3430 cm^{-1} in the outer cell wall were derived from cellulose in the compound middle lamella. Stronger peak intensity at 1600 and 1640 cm^{-1} in the inner layer was considered to be aromatic and phenolic compounds. These results suggested that the inner layer contained not only suberin but also phenolic compounds. Note that the inner layer had an amorphous-like shape (Fig. 5a, b, and d–f), but the suberin aliphatic domain in the inner layer was oval shaped as in the middle layer in radial sections (Fig. 3b, c).

Tensile properties and cell wall components of birch bark

The tensile tests revealed that birch cork in the wet state showed significantly higher extensibility and toughness than in the air-dried and oven-dried states. Birch cork showed a higher Young's modulus in the air-dried and oven-dried states than in the wet state. These results indicated that water plays an important role in stress transfer of birch cork in the tangential direction and, therefore, stress concentration occurs in the dried state. However, suberin, which is the predominant component of the cork cell wall, is highly hydrophobic and is unlikely to interact with water. Therefore, it is reasonable to imagine that the middle layer and compound middle lamella are engaged in bearing tensile stress and stress-transfer between cells. Previous reports using Raman and FTIR spectroscopy indicate that cellulose contributes to bearing the tensile load but lignin does not (Eichhorn et al. 2001; Gierlinger et al. 2006; Salmén and Bergström 2009). Note that significant decrease in toughness did not occur in the air-dried state. Suberin in the outer and inner layer may prevent complete loss of bonding water in the compound middle lamella and middle layer in the air-dried state. Based on insights from previous reports and the present observations, we hypothesized a hierarchical model of the birch cork cell wall (Fig. 8). The lignified layer with a helical arrangement of cellulose microfibrils is sandwiched between two suberized layers. The outer layer is thick

and has a multilayered structure, and the inner layer is thin. In both suberized layers, molecular chains of the suberin aliphatic domains are oriented perpendicular to the suberin lamellae. Under tensile stress in the tangential direction, cellulose microfibrils in the middle layer act like a spring and bear the tensile load. In the wet state, water and cellulose in the compound middle lamellae transfer tensile stress between cells, thus forming a tandemly connected spring. In the dried state, this stress-transferal system does not function well and fewer cells are engaged to bear stress. This results in lower extensibility in the dried state than that in the wet state (Fig. 1). Suberin in the outer and inner layers prevent cellulose in the middle layer and compound middle lamella from losing water so that the bark can bear tensile stress caused by trunk diameter growth.

Comparison of properties between birch and cherry cork

Birch cork shows similar tensile behavior to that of cherry cork reported in previous research (Kobayashi et al. 2018; Xu et al. 1997). This is due to the tangentially elongated cell shape of both birch and cherry cork. However, the tensile strength and toughness of birch cork is lower than that of cherry cork. This can be explained by the larger lumen and thinner cellulosic layer of birch cork compared with those of cherry cork. The deterioration of tensile properties caused by drying is also observed in cherry cork (Kobayashi et al. 2018). However, the deterioration is less significant in birch cork. In birch and cherry cork, cell shapes in the radial section differ substantially. Birch cork cells have a large, oval-shaped lumen, whereas cherry cork cells have a folded shape and small lumen. In addition, cherry cork cell walls show a two-layered structure and a suberized innermost layer is absent (Kobayashi et al. 2018). The presence of the inner layer and a high proportion of the lumen may result in high insulation and drying resistance, and may be the reason for the widespread distribution of birch on the Eurasian continent.

Conclusions

This research investigated the histochemical structure and tensile properties in the tangential direction of birch cork. The birch cork cell wall shows a three-layered structure. The thick outer layer and thin inner layer predominantly consist of suberin. The middle layer mainly consists of lignin, cellulose and other polysaccharides. Tensile tests indicated that birch cork in the wet and air-dried states show higher extensibility and toughness than that in the oven-dried state. These results indicate that cellulose in the middle layer bears tensile loads and that water in the middle layer and compound middle lamella plays an important role in the stress-transferal mechanism. The suberized outer and inner layers may act as hydrophobic barriers and prevent complete water loss to maintain the tensile properties of cork.

Abbreviations

FTIR Fourier-transformed infrared

$KMnO_4$ potassium permanganate

OsO_4 osmium tetroxide

PAS periodic acid–Schiff

PLM polarizing light microscopy

TEM transmission electron microscopy

Declarations

Funding

This research was financially supported by Grants-in-Aid for Scientific Research on Innovative Areas (18H05485).

Conflicts of interest/Competing interests

There is no conflict of interest.

Availability of data and material

Data sharing is not applicable to this article.

Authors' contributions

JS conceived and designed research. SK conducted experiments and wrote the manuscript. All authors read and approved the manuscript.

Acknowledgements

This research was financially supported by Grants-in-Aid for Scientific Research on Innovative Areas (18H05485). The TEM observation was performed in collaboration with the Analysis and Development System for Advanced Materials (ADAM) at the Research Institute for Sustainable Humanosphere, Kyoto University. We thank Robert McKenzie, PhD, from the Edanz Group (https://en-author-services.edanz.com/ac) for editing a draft of this manuscript.

References

Anjos O, Pereira H, Rosa ME (2008) Relation between mechanical properties of cork from *Quercus Suber*. II LATIN AMERICAN IUFRO CONGRESS. La Serena, Chile - Octubre 23-27. In Cd Room

Anjos O, Pereira H, Rosa ME (2010) Tensile properties of cork in the tangential direction: variation with quality, porosity, density and radial position in the cork plank. Materials and Design 31:2085-2090

Bhat KM. 1982. Anatomy, basic density and shrinkage of birch bark. IAWA Bull. n.s. 3:207-213

Ekman R, Eckerman C (1985) Aliphatic carboxylic acids from suberin in birch outer bark by hydrolysis, methanolysis and alkali fusion. Paperi ja Puu. 67:255-273.

Eichhorn SJ, Sirichaisit J, Young RJ (2001) Deformation mechanisms in cellulose fibres, paper and wood. J. Mater. Sci. 36:3129-3135

Gandini A, Neto CP, Silvestre AJD (2006) Suberin: A promising renewable resource for novel macromolecular materials. Prog. Polym. Sci. 31:878-892

Gibson LJ, Easterling KE, Ash MF (1981) The structure and mechanics of cork. Proc. R. Soc. Lond. 377:99-117

Gierlinger N, Schwanninger M, Reinecke A, Burgert I (2006) Molecular changes during tensile deformation of single wood fibers followed by raman microscopy. Biomacromolecules 7:2077-2081

Kobayashi K, Ura Y, Kimura S, Sugiyama J (2018) Outstanding toughness of cherry bark achieved by helical spring structure of rigid cellulose fiber combined with flexible layers of lipid polymers. Adv. Mater. 30:1705315

Pereira H (2015) The rationale behind cork properties: A review of structure and chemistry. Bioresources 10:6207-6229

Reedy MK (1965) Section staining for electron microscopy. Incompatibility of methyl nadic anhydride with permanganates. J. Cell Biol. 26:309-11

Ryser U, Holloway PJ (1985) Ultrastructure and chemistry of soluble and polymeric lipids in cell walls from seed coats and fibres of *Gossypium* species. Planta 163:151-163

Salmén L, Bergström E (2009) Cellulose structural arrangement in relation to spectral changes in tensile loading FTIR. Cellulose 16:975-982

Schmutz A, Jenny T, Amrhein N, Ryser U (1993) Caffeic acid and glycerol are constituents of the suberin layers in green cotton fibres. Planta 189:453-460

Schmutz A, Buchala AJ, Ryser U (1996) Changing the dimensions of suberin lamellae of green cotton fibers with a specific inhibitor of the endoplasmic reticulum-associated fatty acid elongases. Plant Physiol. 11:403-411

Schönherr J, Ziegler H. 1980. Water permeability of *Betula* periderm. Planta 147: 345-354

Serra O, Soler M, Hohn C, Sauveplane V, Pinot F, Franke R, Schreiber L, Prat S, Molinas M, Figueras M (2009) *CYP86A33*-targeted gene silencing in potato tuber alters suberin composition, distorts suberin lamellae, and impairs the periderm's water barrier function. Plant Physiol. 149:1050–1060

Shibui H, Sano Y (2018) Structure and formation of phellem of *Betula maximowicziana* IAWA J. 39:18-36

Sitte P (1962) Zum Feinbau der Suberinschichten im Flaschenkork. Protoplasma. 54:555-559

Teixeira RT, Pereira H (2010) Suberized cell walls of cork from cork oak differ from other species. Microsc. Microanal. 16, 569–575,

Xu X, Schneider E, Chien AT, Wudl F (1997) Nature's high-strength semitransparent film: The remarkable mechanical properties of *Prunus Serrula* bark. Chem. Mater. 9:1906-1908

Yang YP, Zhang Y, Lang YX, Yu MH (2017) Structural ATR-IR analysis of cellulose fibers prepared from a NaOH complex aqueous solution. IOP Conf. Series: Materials Science and Engineering 213:012039

Zhang X, Chen S, Ling Z, Zhou X, Ding DY, Kim YS, Xu F (2016) Method for removing spectral contaminants to improve analysis of raman imaging data. Scientific Reports 7:39891

Figures

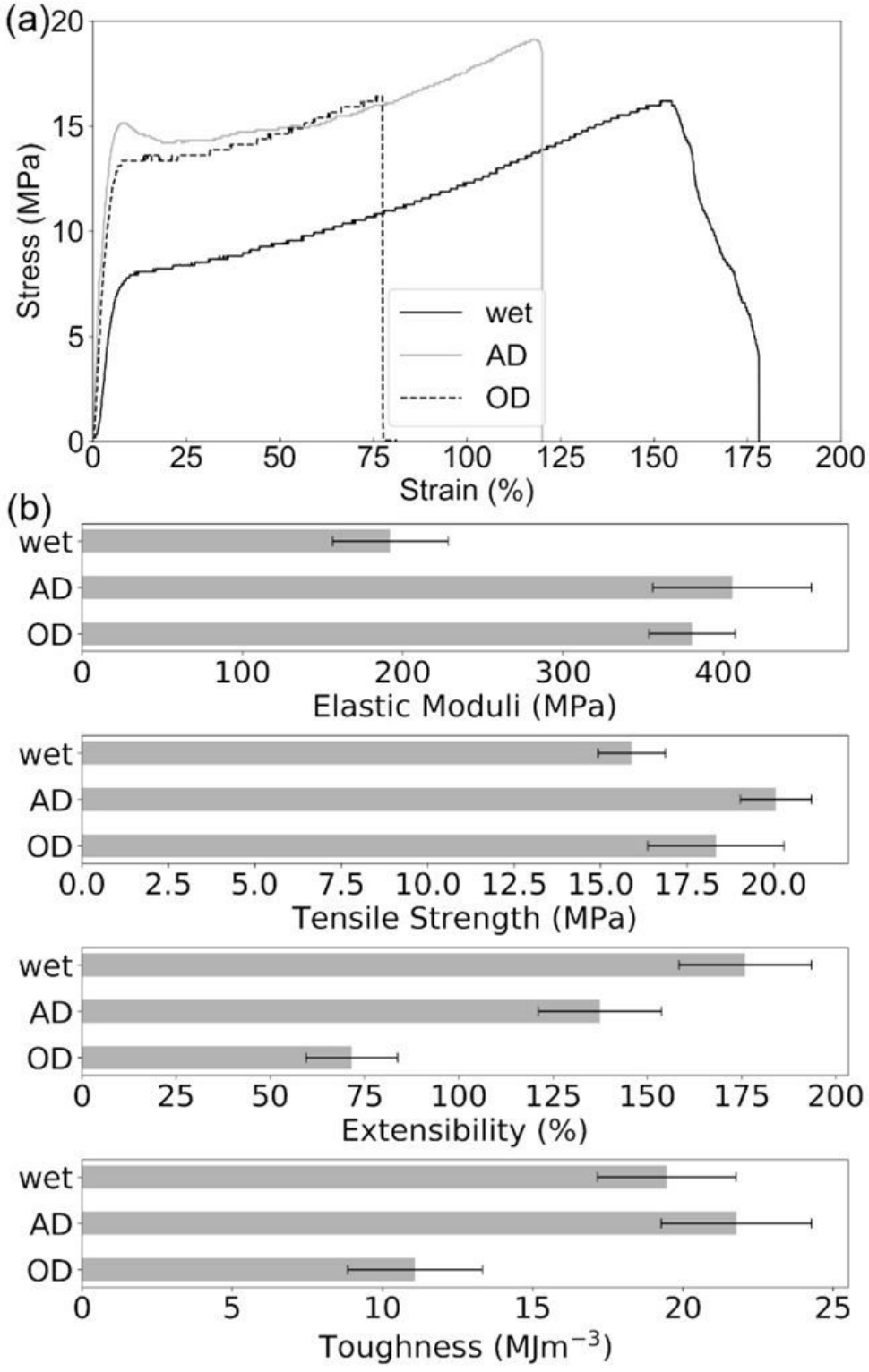

Figure 1

Representative stress-strain curves of tensile tests in the tangential direction of wet-state, air-dried, and oven-dried birch cork (a), and mean value of each tensile parameter (b). Error bars indicate the standard deviation. Tests were performed 10 times for each state. AD air-dried, OD oven-dried

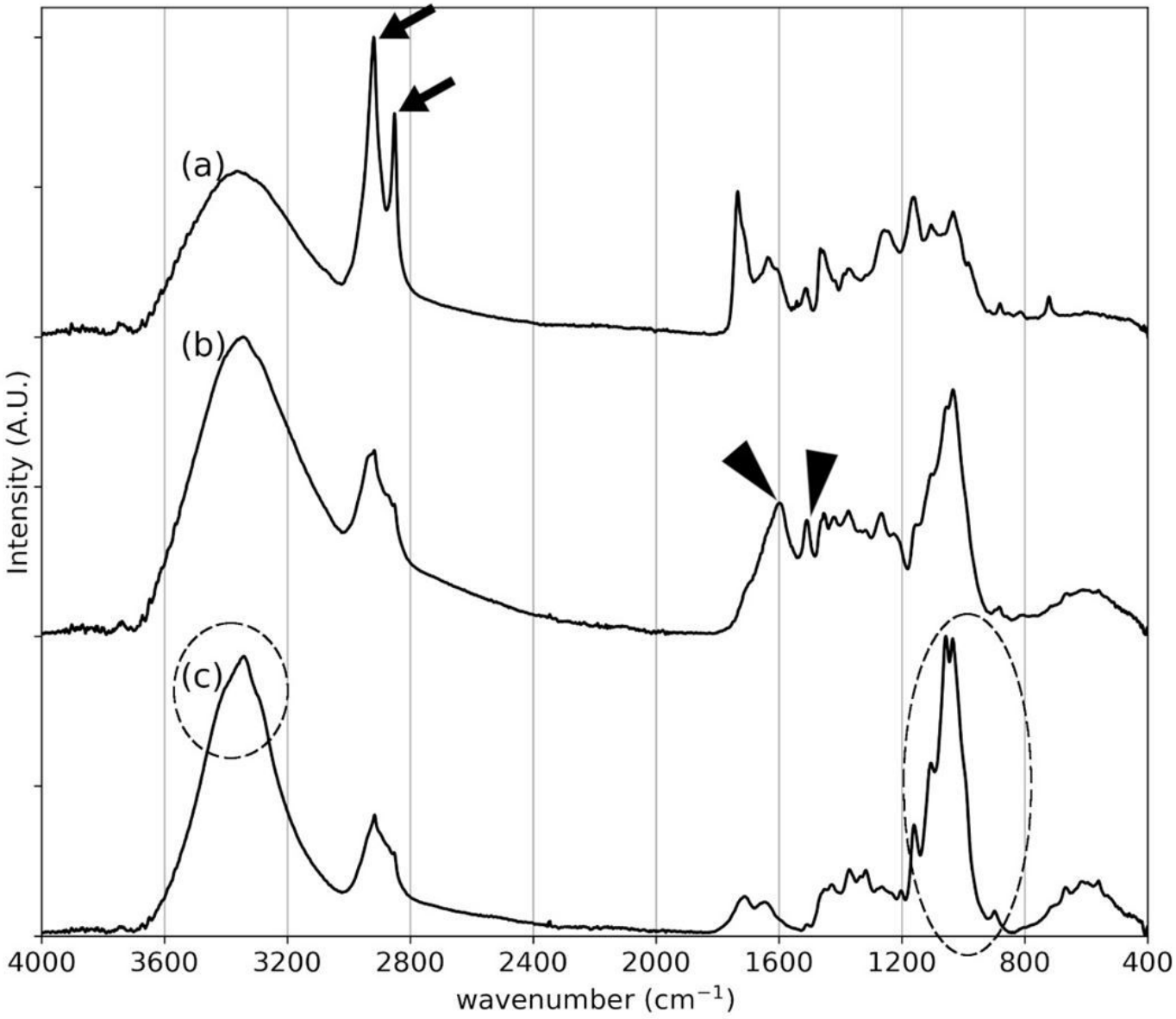

Figure 2

Fourier-transformed infrared spectra of birch cork before chemical treatment (a), after removal of suberin (b), and after removal of suberin and lignin (c). Arrows indicate CH stretching peaks that stem from the suberin aliphatic domain. Arrowheads indicate peaks that stem from aromatic skeleton vibrations of lignin. Ellipses indicate the fingerprint region of cellulose I

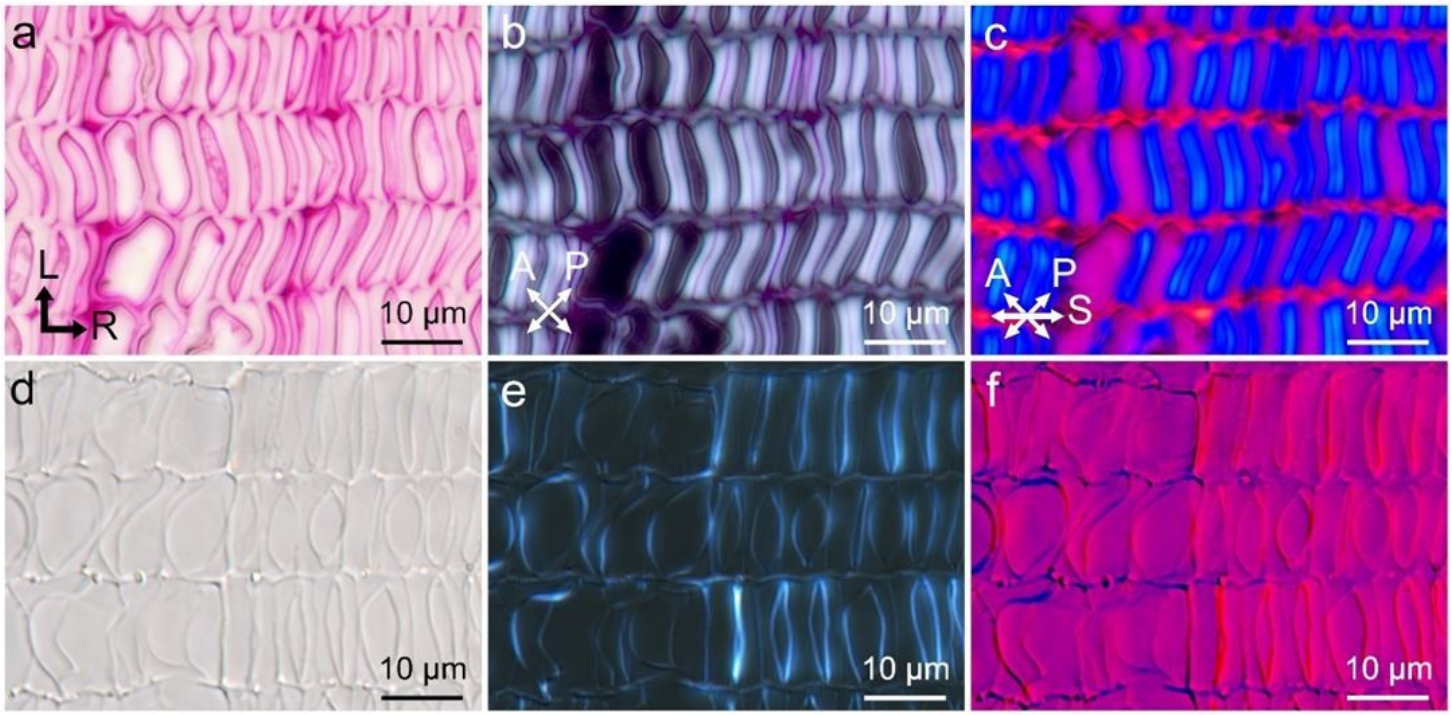

Figure 3

Polarizing light micrographs of radial sections from birch cork stained by the periodic acid–Schiff reaction after bleaching using the Wise method (a–c), and unstained but subject to removal of suberin and lignin (d–f). Sections were observed under opened-Nicol (a, d), crossed-Nicol (b, e), and crossed-Nicol prisms with a retardation plate (c, f). L longitudinal direction, R radial direction, A analyzer, P polarizer, S slow axis

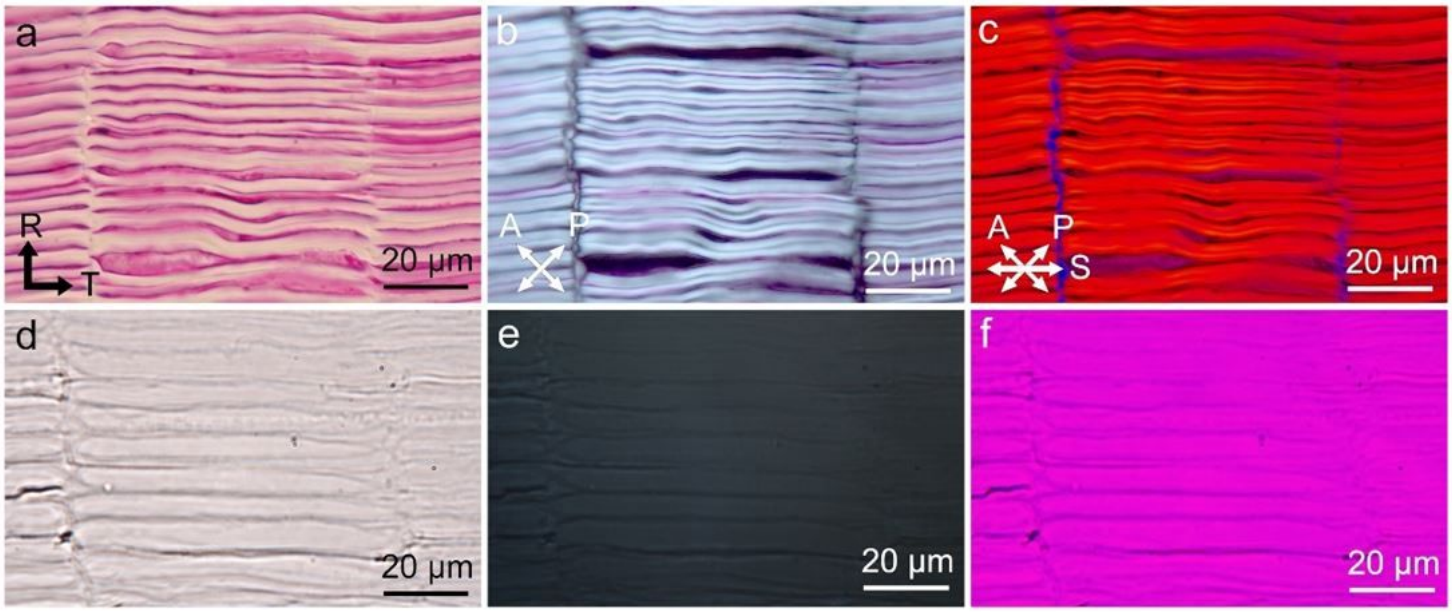

Figure 4

Polarizing light micrographs of transverse sections from birch cork stained by the periodic acid–Schiff reaction after bleaching using the Wise method (a–c), and unstained but subject to removal of suberin and lignin (d–f). Sections were observed under opened-Nicol (a, d), crossed-Nicol (b, e), and crossed-Nicol prisms with a retardation plate (c, f). R radial direction, T tangential direction, A analyzer, P polarizer, S slow axis

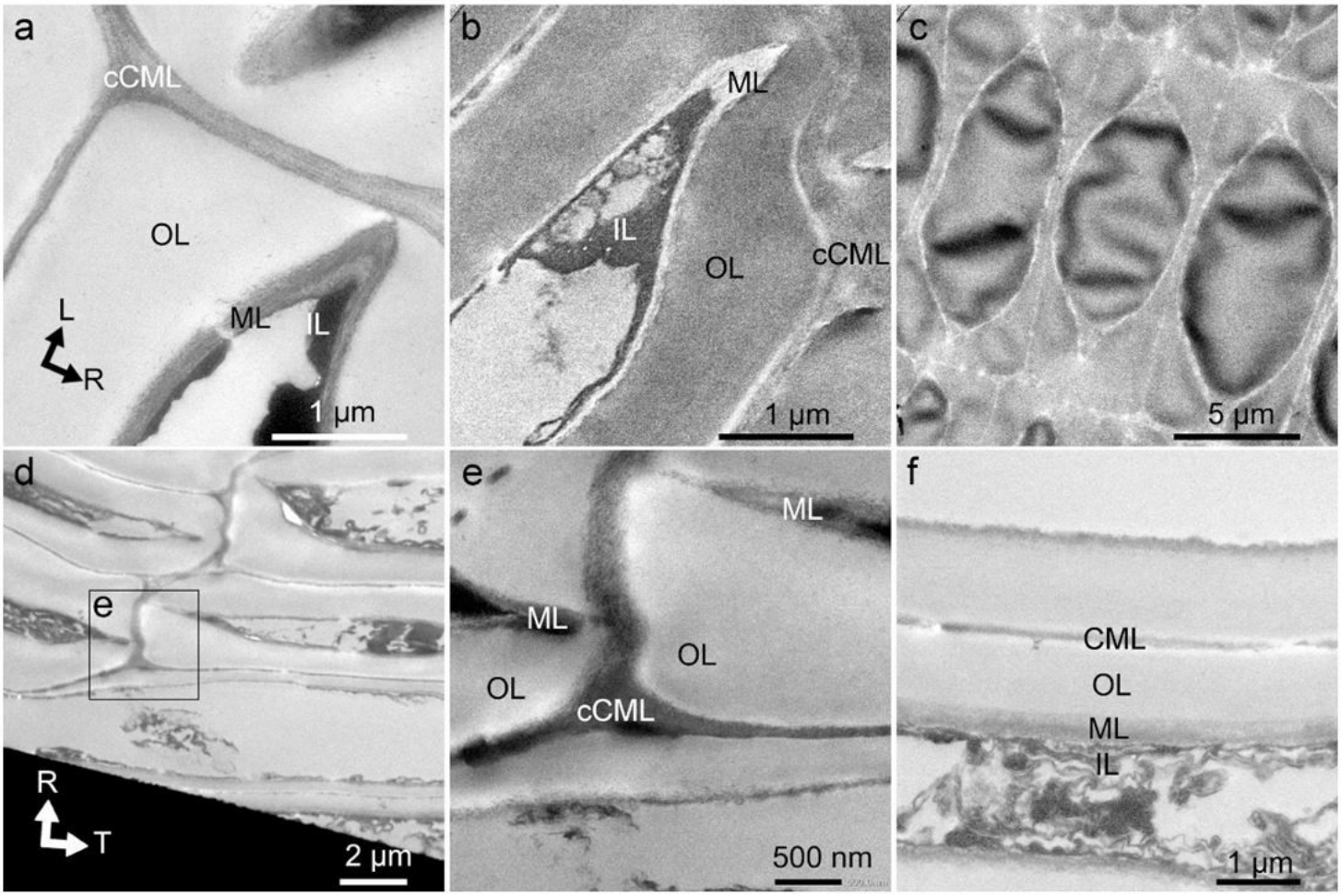

Figure 5

Transmission electron micrographs of KMnO4-stained radial (a–c) and transverse (d–f) sections. Staining was performed before embedding with Spurr resin (b), after embedding with Spurr resin (a, d–f), or after removal of suberin and lignin, and Epon812 resin embedding (c). cCML corner of compound middle lamellae, CML compound middle lamella, OL outer layer, ML middle layer, IL inner layer, L longitudinal direction, R radial direction, T tangential direction

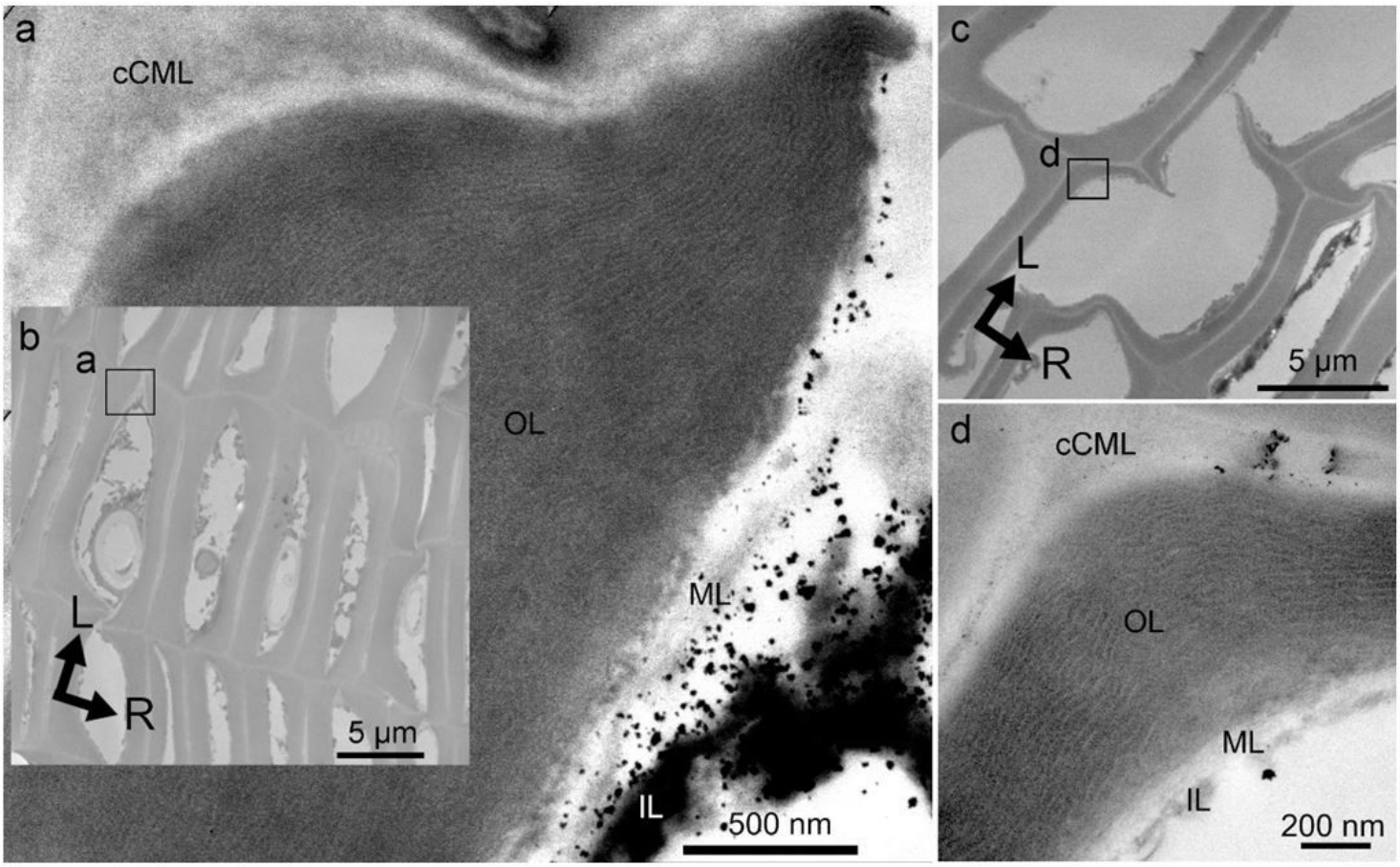

Figure 6

Transmission electron micrographs of OsO4-stained radial section cut from late cork (a, b) and early cork (c, d). Staining was performed before embedding. cCML corner of compound middle lamellae, CML compound middle lamella, OL outer layer, ML middle layer, IL inner layer, L longitudinal direction, R radial direction

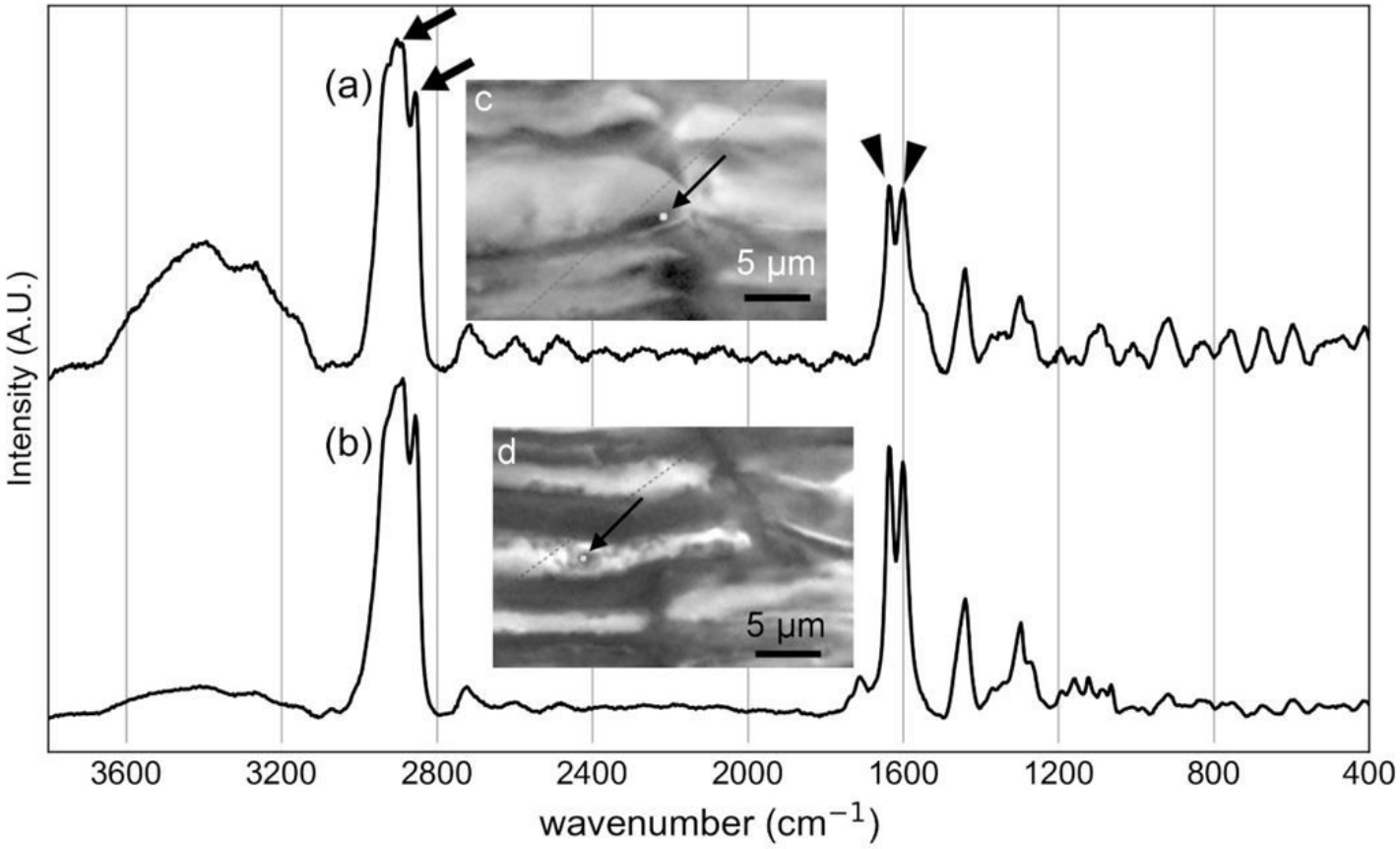

Figure 7

Raman spectra (a, b) of birch cork acquired from the point indicated by arrows in brightfield micrographs (c, d) of a transverse section. Arrows in (a) indicate CH stretching bands that stem from the suberin aliphatic domain. Arrowheads indicate peaks that stem from the aromatic ring.

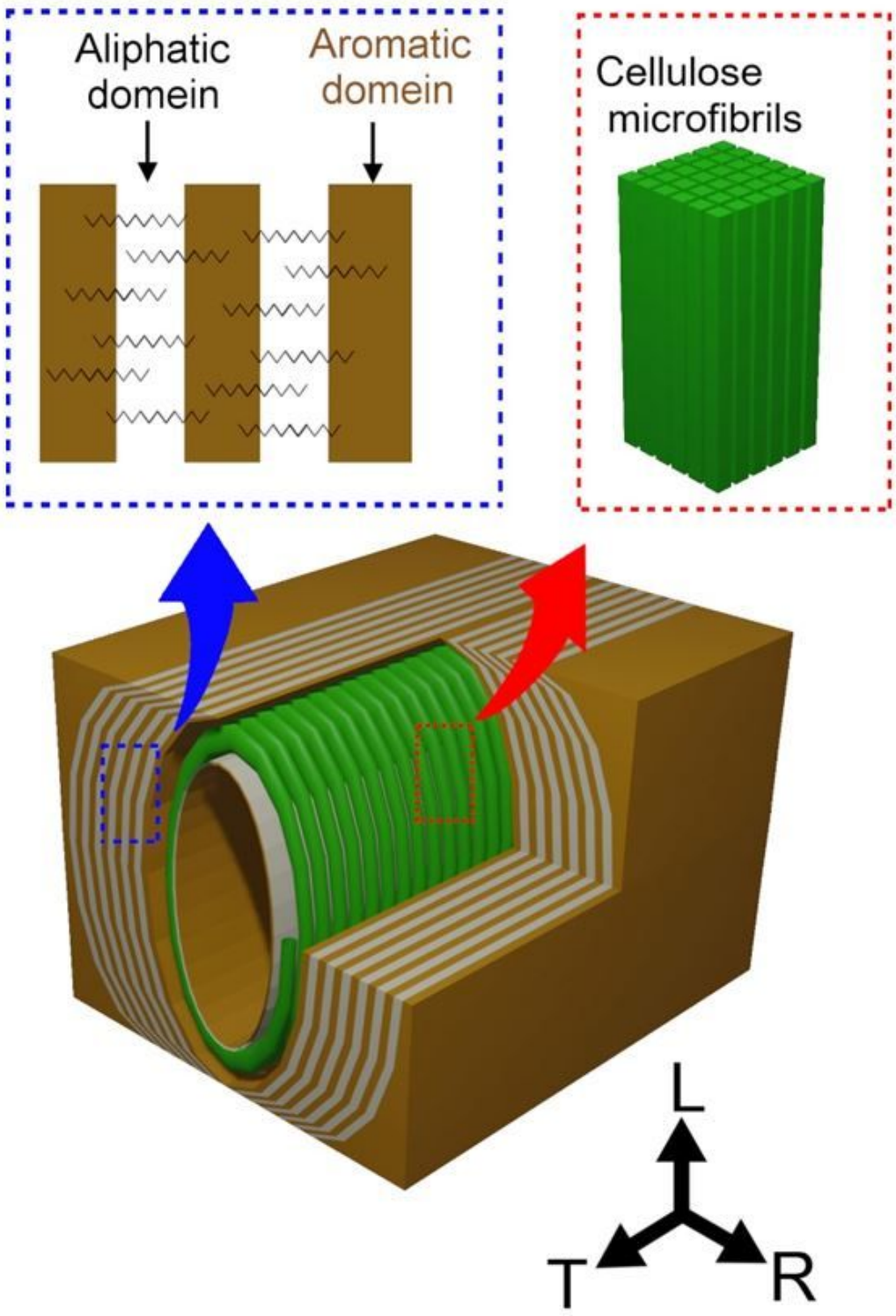

Figure 8

Schematic illustration of the birch cork cell wall. L longitudinal direction, R radial direction, T tangential direction.